Nanotechnology Perceptions
ISSN 1660-6795
www.nano-ntp.com

Characterization Of Self-Compacting Concrete Incorporating Municipal Solid Waste Ash And Waste Foundry Sand

Gurpreet Singh Sidhu

Department of Civil Engineering, Punjabi University, Patiala, Punjab, INDIA
gurpreet.sidhu69@gmail.com

The importance of adopting environmentally sustainable practices and regulations that can improve productivity, enhance concrete performance, and reduce energy consumption is increasingly known-by the construction industry. The development of self-compacting concrete (SCC) adding 20% municipal solid waste ash (MSWA) as a supplementary additive is investigated in this study. Appropriate treatment, recycling, or safe disposal is required for MSWA, which results from incinerating domestic and commercial waste, because various minerals, metals, glass particles, and other contaminants are present in it. Cementitious composites can incorporate MSWA as an additive because of its pozzolanic characteristics. In this study, waste waste foundry sand(WWFS) replaced 20%, 40%, and 60% of the fine aggregate in SCC. To examine the influence of MSWA and WFS on the fresh, mechanical, and durability properties of SCC. Fresh state characteristics were found using slump flow, L box, U box, and V funnel tests to characterize workability and passing ability, while compressive strength tests were done to quantify the material's mechanical performance. Durability was evaluated using four tests: rapid chloride permeability to measure how easily ions pass through, mass loss to track material deterioration, and abrasion resistance to evaluate surface wear. The results show that adding waste foundry sandto self compacting concrete helps increase its strength (for example, compressive strength) and improves durability by reducing cracking and permeability, leading to better long-term performance.

Keywords: Self-compacting concrete, Municipal Solid Waste Ash, Foundry Sand, Compressive strength, Abrasion.

1. Introduction

Significant amounts of natural resources are consumed, and energy use and carbon dioxide emissions are substantially increased, by large scale concrete production; however, the world uses concrete more than any other construction material. Moreover, the cement and concrete sector faces mounting pressure to curtail its environmental footprint through clinker reduction, the deployment of supplementary cementitious materials, waste valorization, and the adoption of efficient concrete technologies [1 4]. In this context, SCC has emerged as an advanced construction material owing to its capacity to flow by its self-weight to complete formwork properly, pass through densely congested reinforcement, and achieve adequate consolidation without mechanical vibration, thereby enhancing placement efficiency and reducing on site labor and noise [5 7]. Eliminating vibration can reduce labor needs, shorten construction time, reduce noise pollution, and cut defects from poor compaction, while improving surface finish and structural quality in real world settings [5,8]. Slump flow, T500, V funnel, L box, and U box tests commonly evaluate filling ability, passing ability, viscosity, and segregation resistance; according to EFNARC guidelines, these properties mainly govern the performance of SCC [6].

The sustainability of SCC can be increased by using industrial, municipal, and agricultural wastes such as fly ash, slag, recycled glass, plastics, or crop residues as cement like additives or to replace natural aggregates like sand and gravel. Pore refinement, long term strength development, and durability can be improved when supplementary cementitious materials are properly proportioned, and the consumption of ordinary Portland cement is reduced by their use [9 11]. Municipal solid waste ash (MSWA), from incinerating household, commercial, and municipal waste, could be used in cementitious composites. MSWA typically contains oxides of calcium, silica (silicon dioxide), alumina (aluminum oxide), and iron, and also includes glassy phases, unburnt particles, various salts, and small amounts of trace metals [12 15]. Owing to its heterogeneous composition and the potential presence of heavy metals or soluble salts, MSWA requires comprehensive characterization, suitable treatment, and safe utilization before being incorporated into concrete, particularly in real world settings [13,16]. Contributing to waste abatement and the transition to circular construction, processed municipal solid waste incineration ash can be employed as a partial cement replacement or mineral additive, provided that researchers rigorously control its chemical composition, fineness, leaching behaviour, and pozzolanic activity, as reported by previous studies [12,14,17 19].

Efforts to replace cement are underway, and the depletion of natural river sand has become a critical issue for sustainable concrete production. Continuous extraction of natural sand causes environmental degradation, riverbed instability, and increased material cost. Ferrous and non-ferrous metal casting industries produce waste foundry sand (WFS), also called waste waste foundry sand or used foundry sand. It is mostly made of good silica sand and is reused several times in moulding operations before being discarded in real world settings [20 22]. WFS has been studied as a part replacement for natural fine aggregate in conventional mixture and SCC; it has fine particle size, a silica rich composition, and fairly uniform grading [21 24]. On top of that, the performance of WFS concrete depends on the type of foundry process, binder residues, clay content, particle shape, fineness, and contaminants present in the waste sand [20,25]. Several researchers have reported that modest levels of waste foundry sand substitution can preserve or even enhance mechanical properties, whereas excessive replacement tends to impair workability and increase water demand owing to the presence of finer particles and residual binders.

Using MSWA as a cementitious additive and waste foundry sand to replace fine aggregate offers a promising path to sustainable SCC. This integrative approach can concurrently curtail cement consumption, attenuate the extraction of natural sand, and redirect municipal and industrial wastes away from landfills in real world settings. Nevertheless, the combined influence of MSWA and WFS on fresh, mechanical, and durability parameters of SCC requires systematic investigation because SCC is highly sensitive to changes in powder content, fine aggregate grading, paste volume, and water-to-binder ratio [6,7,28]. In particular, the incorporation of waste materials may alter flowability, passing ability, viscosity, segregation resistance, compressive strength, chloride ion penetration, water absorption, mass loss, and abrasion resistance.

2. Experimental Programme

2.1 Materials

This study used 43-grade Ordinary Portland Cement conforming to BIS 8112:1989. Locally sourced river sand, satisfying Zone II grading requirements of BIS 383:1970, served as the fine aggregate, with a specific gravity of 2.66 and fineness modulus of 2.70. Crushed coarse aggregate of 12 mm nominal maximum size was used, having a specific gravity of 2.69 and fineness modulus of 5.94.

Waste foundry sand was obtained from Jindal Steel, Hisar. It was light brown in colour, with a specific gravity of 2.39. Its particle-size distribution was determined through sieve analysis. Chemically, it mainly consisted of silica, alumina, and calcium oxide.

Fig: 2.1 Grading of river sand and foundry sand

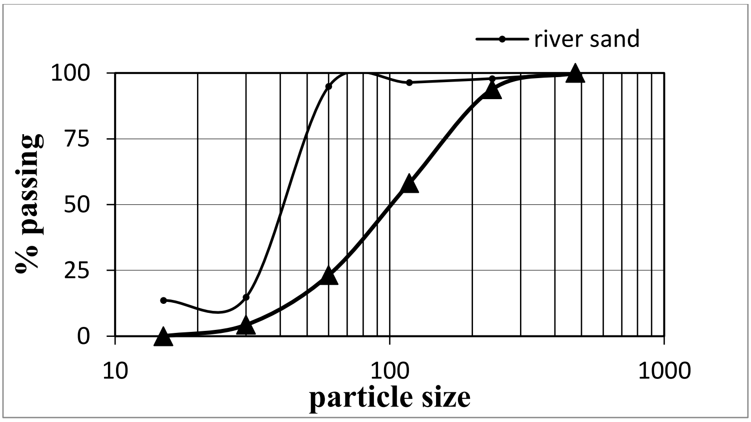

Table:2.1 Passing percentage of river sand and foundry sand

Particle size	River sand % passing	Waste foundry sand% passing	Difference
150 micron	14%	0%	River sand has more fine particles
300 micron	14%	4%	River sand still slightly finer
600 micron	95%	23%	Big difference: river sand is much finer here
1.18 mm	96–100%	58%	River sand is almost fully passing; waste foundry sand is still much coarser
2.36 mm	98–100%	94%	Both are mostly passing
4.75 mm	100%	100%	Both sands fully pass

2.5 Municipal Solid Waste Ash (MSWA)

A nearby dumping site of Patiala city is the source for the collection of MSWA

2.6 Admixture

Aura-Mix 400 is an advanced, chloride-free super-plasticizing admixture developed from modern polycarboxylate-based technology with extended side-chain structures. It appears bright yellow and has an approximate pH value of 6.0.

3. Mix Proportions

The SCC mix proportions were developed through repeated laboratory trial batches. The reference mixture was prepared to attain a 28-day CS of 25 MPa. For the modified mixes, river sand was replaced with waste foundry sand (WFS) at 20%, 40%, and 60% replacement levels. Municipal solid waste ash (MSWA) was also added at 20% of the cement weight. The water percentage was same in all mixtures, while a superplasticizer equal to 1% of the cement mass was used to improve flowability and achieve the appropriate fresh parameters of SCC. In the Table 3.1 Mixture ID used as SC Concrete-0 [0% WFS replaced], SC Concrete-20[20% WFS replaced], SC Concrete-40[40% WFS replaced], SC Concrete-60[60% WFS replaced]

Table: 3.1 Mixture values of SCC with WFS

Mixture ID	**SC Concrete-0**	**SC Concrete-**	**SC Concrete-**	**SC Concrete-**
Cement (kg/m^3)	360	360	360	360
MSWA (kg/m^3)	72	72	72	72
Sand (kg/m^3)	950	760	570	380
WFS (kg/m^3)	0	190	380	570
Coarse aggregates (kg/m^3)	820	820	820	820
Water (liters)	195	195	195	195

4 Result and Discussions

4.1 Fresh SCC Properties

SC Concrete-0 is used as the control mixture. SC Concrete-20 shows almost the similar slump flow and V-funnel time as the control, while its L-box ratio increases from 0.90 to 0.92 and its U-box difference decreases from 35 mm to 32 mm. This suggests that SC Concrete-20 has slightly better passing ability and filling behavior than the control mix.

Results of fresh SCC properties are presented in Fig.4.2 Because the four properties have different units, then, normalized the values using SC Concrete-0 as 100%**.** This makes the mixtures easier to compare on one graph.SC Concrete-40 gives the highest slump value, increasing from 750 mm to 760 mm. Its L-box value also improves slightly. However, the V-funnel time increases from 11 seconds to 12 seconds, showing that the mix flows a little more slowly through the funnel. Its U-box value remains the same as the control.

SC Concrete-60 shows a reduction in slump from 750 mm to 730 mm, indicating lower flowability compared with SC Concrete-0. Its V-funnel and L-box values are similar to the control, while the U-box difference decreases slightly to 33 mm. Overall, SC Concrete-60 still behaves close to the control mix, but its lower slump suggests reduced fresh workability. Overall, SC Concrete-20 appears to give the most balanced fresh-property performance**,** because it maintains the flow time, slightly improves the L-box ratio, and reduces the U-box height difference compared with SC Concrete-0.

Fig:4.1 Image of tests performing (U-box and Slump flow)

Fig. 4.2 Fresh property results of SCC mixtures

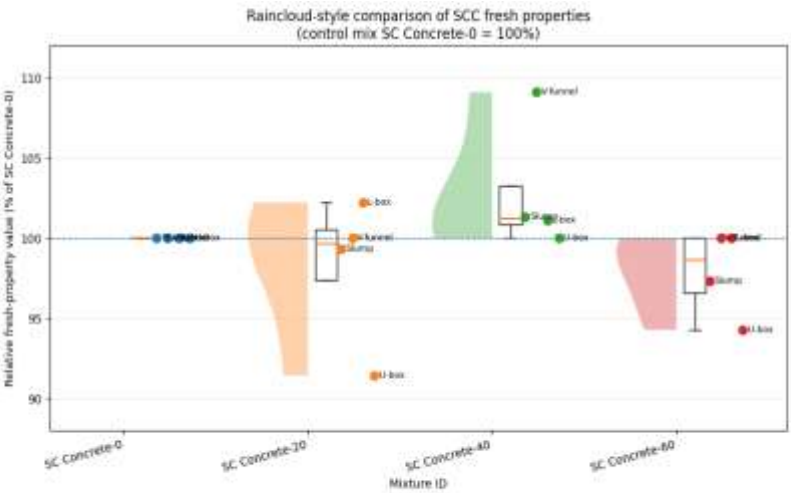

4.2 Compressive Strength of SCC Mixtures

SC Concrete-0 as the reference mix, The Fig.4.3 shows that adding higher SC replacement levels increased compressive strength at all curing ages. The improvement is most noticeable at 28 and 91 days**,** especially for SC Concrete-40 and SC Concrete-60**.**

Table:4.1 Percentage increase in CS compared with SC Concrete-0

Age	SC Concrete -0	SC Concrete -20	% Increase	SC Concrete -40	% Increase	SC Concrete -60	% Increase
7 days	19.70	21.07	6.95%	22.20	12.69%	24.70	25.38%
28 days	25.10	27.10	7.97%	30.20	20.32%	32.10	27.89%
91 days	27.13	29.60	9.10%	33.10	22.01%	34.53	27.28%
365 days	31.10	31.80	2.25%	34.30	10.29%	35.70	14.79%

Fig:4.3 CS Development of SCC Concrete Mixture

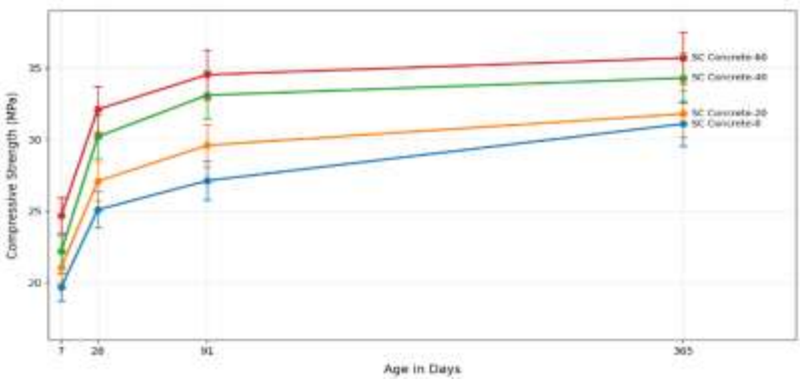

At 7 days, all modified mixes performed better than the reference mix. A 25.38% increase compared with SC Concrete 0 was shown by SC Concrete 60, which exhibited the highest early age strength.

At 28 days, the strength gain became more significant. SC Concrete 60 again showed the largest improvement, with an increase of 27.89%, followed by SC Concrete 40, which increased by 20.32%.

At 91 days, the same trend continued. SC Concrete-60 achieved the maximum strength of 34.53 MPa, giving a 27.28% increase over the reference mix. This indicates strong later-age strength development.

The percentage disparity narrowed; nevertheless, at 365 days higher strength than SC Concrete 0 was still exhibited by all mixes. SC Concrete 60 remained the best performing mix with a 14.79% increase, while SC Concrete 20 showed only a small improvement of 2.25% in everyday situations.

Overall, SC Concrete 60 showed the highest compressive strength at every curing age, making it the best performing mixture in this dataset in real world settings. The strength benefit peaked at 91 days and attenuated by 365 days.

4.3 Rapid Chloride Permeability Test

According to ASTM C1202, RCP is classified by six-hour charge passed: >4000 C (high), 2000 4000 C (moderate), 1000 2000 C (low), 100 1000 C (very low), and <100 C (negligible). All the values, from 1347 to 1588 coulombs, are within the low chloride ion penetrability range in real world settings.

Fig:4.4. RCPT results of SC Concrete mixtures

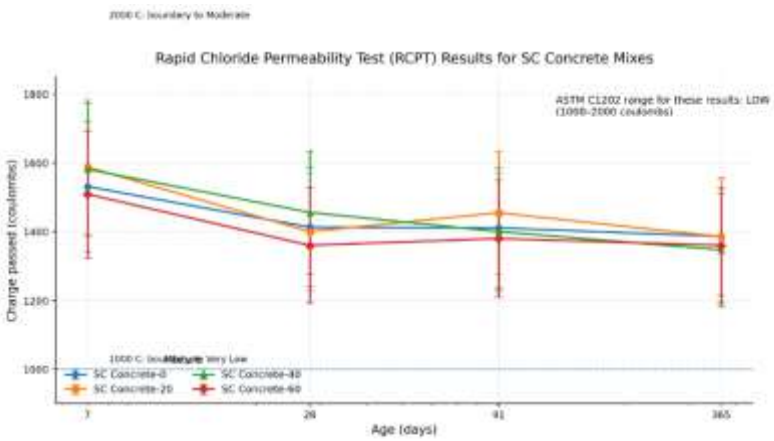

As the mixtures age, they generally pass less electrical charge, indicating improved resistance to chloride ion movement as the concrete gains strength and its pore structure becomes tighter. Results are shown in Fig. 4.4 SC Concrete 40 is lowest at 365 days (1347 C), while SC Concrete 60 is best at 28 and 91 days. Although none of the mixtures attains the "very low" designation, all remain comfortably below the ASTM "moderate" threshold of 2000 C in practice.

4.4 Sulphate Resistance (SR)

Sulphate resistance tests were conducted as per ASTM C1012-10. At 7 days, the percentage change for all mixes is very small, showing that the effect of sulphate at early ages is limited and not yet significant. Approximately between 1.5% and 3.8% is the gradual increase in percentage change shown by all SCC mixes from 28 to 91 days. The increase becomes clearer at 365 days, where the values range from 7.0% to 8.0%. This indicates that the effect of 10% magnesium sulphate becomes more noticeable with longer immersion time.

At 365 days, SC-Concrete-0 shows the lowest percentage change, 7.0%, followed by SC-Concrete-60 at 7.5%, SC-Concrete-40 at 7.8%, and SC-Concrete-20 at 8.0%. Based only on the plotted percentage change, SC-Concrete-0 shows the best resistance to strength variation under magnesium sulphate exposure, while SC-Concrete-20 shows the highest change at one year. However, because the difference among mixes is only about 1%, the mixes behave fairly close to each other under sulphate immersion.

Fig:4.5 Percentage loss of Compressive Strength

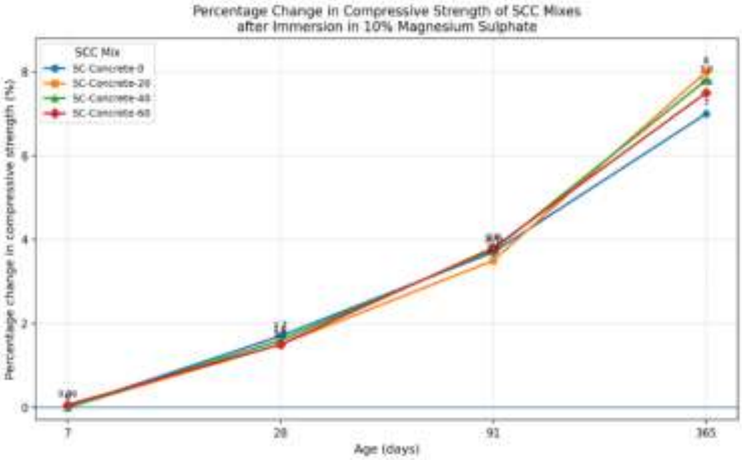

4.5 Abrasion Resistance

The horizontal axis is wear time in minutes**,** and the vertical axis is wear depth in mm. All curves increase with time, which means abrasion depth increases as rubbing duration increases. Results are shown in Fig.4.6. Abrasion resistance of SCC calculated according to BIS: 1237-2012.

The 7-day samples show the highest wear, meaning lower early-age abrasion resistance. The 365-day samples show the lowest wear**,** meaning better long-term abrasion resistance due to continued concrete hardening.

Fig: 4.6. Abrasion Wear Depth vs Wear Time for SC Concrete

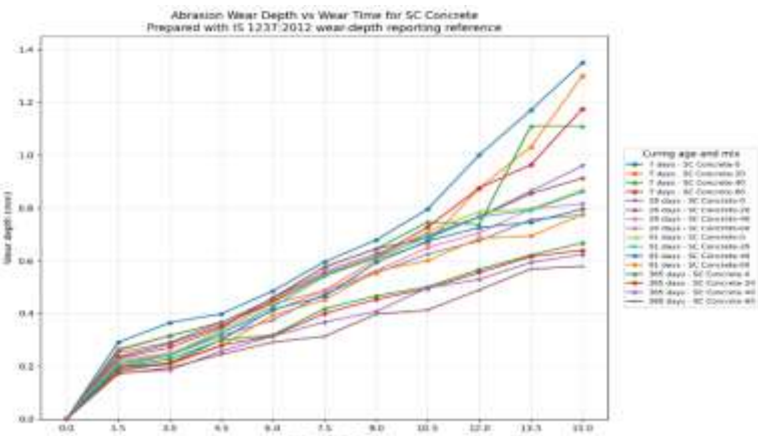

Table:4.2. Average wear depth of all mixes

Curing age	SC-0 avg wear	SC-20 avg wear	SC-40 avg wear	SC-60 avg wear	Best mix
7 days	0.648	0.577	0.574	0.566	SC-60
28 days	0.530	0.522	0.474	0.453	SC-60
91 days	0.505	0.496	0.465	0.439	SC-60
365 days	0.389	0.377	0.359	0.333	SC-60

SC Concrete-60 gives the best abrasion resistance at every curing age**,** because it has the lowest average wear depth. The best overall result is 365 days – SC Concrete-60**,** with average wear of 0.333 mm and final 15-minute wear depth of 0.579 mm**.**
The highest final wear depth in your data is 1.350 mm for 7 days – SC Concrete-0**,** which is still below the 2.0 mm heavy-duty average wear limit and 3.5 mm general-purpose average wear limit stated in IS 1237:2012

5. Two-way ANOVA screening results
Method used: **two-way ANOVA without replication**, with factors:

- Factor 1: Age
- Factor 2: SCC mix type

Table: 5.1 Statical Analysis (ANOVA)

Property	Factor	F-value	p-value	Interpretation
Compressive strength	Age	171.69	<0.001	Highly significant
Compressive strength	Mix type	51.12	<0.001	Highly significant
RCPT	Age	45.51	<0.001	Highly significant
RCPT	Mix type	4.64	0.032	Significant
Sulphate strength change	Age	637.09	<0.001	Highly significant
Sulphate strength change	Mix type	0.26	0.855	Not significant
Abrasion final wear depth	Age	82.95	<0.001	Highly significant
Abrasion final wear depth	Mix type	2.48	0.127	Not significant at 5% level

5.1 Statistical interpretation
Notably, the analysis of variance demonstrates that age exerts a statistically significant effect on each of the four assessed properties. This means the curing age has a strong influence on

strength development, on chloride permeability, on strength changes due to sulphate exposure, and on resistance to abrasion.
For compressive strength, both age and mix type were highly significant. This substantiates the graphical observation that SC Concrete-40 and SC Concrete-60 augmented strength relative to the control mix, thereby confirming their superior performance.
For RCPT, age was highly significant and mix type was also significant. This indicates that chloride permeability was affected by both curing duration and SCC mix composition. SC Concrete-60 showed the best long-term chloride resistance.
On top of that, age was highly significant for sulphate resistance, but mix type was not statistically significant. It is meant that exposure/curing age, rather than SC percentage, mainly controlled the increase in strength after sulphate immersion.
Age strongly influenced abrasion resistance; mix type was not significant at the 5% level. Although SC 40 and SC 60 generally produced lower wear depths, the estimated data suggest that curing age (the time allowed for curing) had a stronger influence on wear than the differences in mix composition.

Table: 5.2 Best-performing mix by property

Property	**Better direction**	**Best mix from graph**	**Reason**
Compressive strength	Higher is better	SC-60	Highest strength at all ages
RCPT	Lower is better	SC-60	Lowest charge passed at 365 days
Sulphate resistance	No strength loss; stable/gain preferred	SC-20 / SC-40	Highest positive strength changes at 365 days
Abrasion resistance	Lower wear depth is better	SC-60 at 365 days	Lowest final wear depth

6. FOURIER TRANSFORM INFRARED SPECTROSCOPY

The FTIR spectra of the SC samples with concentrations of 0%, 20%, 40%, and 60% showed several characteristic absorption peaks, indicating the presence of different functional groups and chemical constituents within the material. These variations in absorption bands provide insight into the structural composition of the samples

Fig.6.1 FTIR Spectra of concrete sample (SC-0%, 20%, 40% and 60%) at 28-day

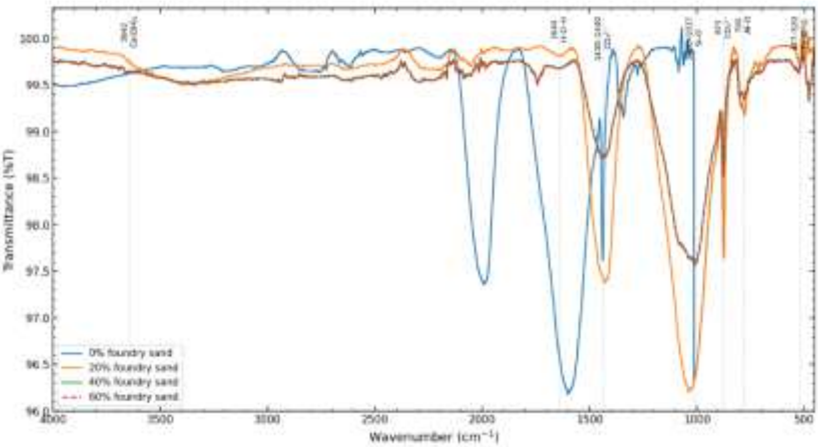

Table: 6.1 Findings from FTIR Spectra

Phase / band	FTIR window used	Main interpretation
$Ca(OH)_2$ / portlandite	3620–3665 cm^{-1}	Very weak in all samples; peak near 3640 cm^{-1} is the expected portlandite OH band.
Si–O / C–S–H + quartz	900–1120 cm^{-1}	Strongest structural band. 20% replacement gave the highest relative Si–O area; 40% and 60% were lower than 0%. C–S–H bands are commonly around 1000–950 cm^{-1}, and Si–O stretching can shift with C–S–H polymerization
Al–O / aluminosilicate	700–830 cm^{-1}	0% and 20% are similar; 40% and 60% are lower. Aluminate phases show several Al–O bands in this region, but overlap with carbonate/silicate bands is possible.
Fe–O / ferrite low-frequency region	450–600 cm^{-1}	40% and 60% show a stronger low-wavenumber band near 477 cm^{-1}.
Carbonate CO_3^{2-}	~1430, 875, 710 cm^{-1}	Clear carbonation/calcite-type bands appear, especially the ~1430 cm^{-1} band. Concrete FTIR commonly shows $CaCO_3$ at ~1410, 872, and 710 cm^{-1}.

7. CONCLUSION

- SCC fresh parameters satisfy the EFNARC values of all the mixtures are within the limits
- The compressive strength graph shows strength rose with curing age for all mixes. SC-60 achieved the highest strength at all ages, followed by SC-40, SC-20, and SC-0. After 365 days of curing, SC 60 reached approximately 35.7 MPa in compressive strength, compared with about 31.0 MPa for the control mix. This indicates that increasing SC content improved long-term strength development.

- The RCPT graph depicts a decline in charge passed with age, indicating reduced chloride ion permeability. Lower RCPT values indicate better resistance to chloride penetration. The densest and least permeable matrix among the mixes is suggested by the lowest long term charge passed, about 1340 coulombs at 365 days, which was recorded for SC 60.
- The sulphate resistance graph displays positive percentage changes in compressive strength after immersion in magnesium sulphate solution, indicating an increase in strength following such exposure. The increase became larger with age for all mixes. At 365 days, SC 20 manifested the largest percentage increase, approximately 8.0%, whereas SC 40, SC 60, and SC 0 recorded increases of 7.8%, 7.5%, and 7.0%, respectively. Because the graph shows strength gains, none of the mixes showed clear compressive strength loss during the plotted period.
- The abrasion resistance graph shows wear depth increased with wear time but decreased sharply with curing age. Lower wear depth means better abrasion resistance. At 7 days, wear depth was relatively high, especially for SC-0. At 365 days, all mixes showed much lower wear depth, with SC-60 giving the lowest final value of about 0.58 mm. This indicates that prolonged curing significantly augmented surface hardness; it concomitantly enhanced abrasion resistance.
- Overall, curing age is the strongest factor affecting all four properties. At the same time, SC replacement clearly improved compressive strength and chloride resistance, while its effect on sulphate strength change and abrasion depth was smaller than that of age.

References

1. G. Sidhu, R. Siddique, Effect of iron slag as partial replacement of fine aggregates on the durability characteristics of self-compacting concrete, Construction and building Materials, Volume 128, (2016) 88-95.
2. R.M. Andrew, Global CO_2 emissions from cement production, Earth System Science Data, 10 (2018) 195–217.
3. M.C.G. Juenger, R. Siddique, Recent advances in understanding the role of supplementary cementitious materials in concrete, Cement and Concrete Research, 78 (2015) 71–80.
4. K.L. Scrivener, V.M. John, E.M. Gartner, Eco-efficient cements: Potential economically viable solutions for a low-CO_2 cement-based materials industry, Cement and Concrete Research, 114 (2018) 2–26.
5. H. Okamura, M. Ouchi, Self-compacting concrete, Journal of Advanced Concrete Technology, 1(1) (2003) 5–15. https://doi.org/10.3151/jact.1.5
6. EFNARC, The European Guidelines for Self-Compacting Concrete: Specification, Production and Use, European Federation for Specialist Construction Chemicals and Concrete Systems, 2005.
7. H.J.H. Brouwers, H.J. Radix, Self-compacting concrete: Theoretical and experimental study, Cement and Concrete Research, 35(11) (2005) 2116–2136. https://doi.org/10.1016/j.cemconres.2005.06.002
8. C.I. Goodier, Development of self-compacting concrete, Proceedings of the Institution of Civil Engineers – Structures and Buildings, 156(4) (2003) 405–414.
9. R. Siddique, Waste materials and by-products in concrete, Springer, Berlin, 2008.

10. P.K. Mehta, P.J.M. Monteiro, Concrete: Microstructure, Properties, and Materials, 4th ed., McGraw-Hill Education, New York, 2014.
11. K. Celik, M.D. Jackson, M. Mancio, C. Meral, A.H. Emwas, P.K. Mehta, P.J.M. Monteiro, High-volume natural volcanic pozzolan and limestone powder as partial replacements for Portland cement in self-compacting concrete, Cement and Concrete Composites, 45 (2014) 136–147.
12. A.M. Joseph, R. Snellings, P. Nielsen, S. Matthys, N. De Belie, Pre-treatment and utilisation of municipal solid waste incineration bottom ashes towards a circular economy, Construction and Building Materials, 260 (2020) 120485. https://doi.org/10.1016/j.conbuildmat.2020.120485
13. J.E. Aubert, B. Husson, A. Vaquier, Use of municipal solid waste incineration fly ash in concrete, Cement and Concrete Research, 34(6) (2004) 957–963. https://doi.org/10.1016/j.cemconres.2003.11.002
14. N.M. Alderete, A.M. Joseph, P. Van den Heede, S. Matthys, N. De Belie, Effective and sustainable use of municipal solid waste incineration bottom ash in concrete regarding strength and durability, Resources, Conservation and Recycling, 167 (2021) 105356. https://doi.org/10.1016/j.resconrec.2020.105356
15. K. Rübner, F. Haamkens, O. Linde, Use of municipal solid waste incinerator bottom ash as aggregate in concrete, Quarterly Journal of Engineering Geology and Hydrogeology, 41(4) (2008) 459–464. https://doi.org/10.1144/1470-9236/07-036
16. M. Vaičienė, E. Simanavičius, The effect of municipal solid waste incineration ash on the properties and durability of cement concrete, Materials, 15(13) (2022) 4486. https://doi.org/10.3390/ma15134486
17. A.M. Joseph, R. Snellings, P. Van den Heede, S. Matthys, N. De Belie, The use of municipal solid waste incineration ash in various building materials: A Belgian point of view, Materials, 11(1) (2018) 141. https://doi.org/10.3390/ma11010141
18. J. Li, Municipal solid waste incineration ash-incorporated concrete: One step towards environmental justice, Buildings, 11(11) (2021) 495. https://doi.org/10.3390/buildings11110495
19. R.K. Dhir, J. de Brito, C.J. Lynn, R.V. Silva, Sustainable Construction Materials: Municipal Incinerated Bottom Ash, Woodhead Publishing, Cambridge, 2017.
20. R. Siddique, G. Singh, Utilization of waste foundry sand (WFS) in concrete manufacturing, Resources, Conservation and Recycling, 55(11) (2011) 885–892. https://doi.org/10.1016/j.resconrec.2011.05.001
21. R. Siddique, G. de Schutter, A. Noumowe, Effect of used-foundry sand on the mechanical properties of concrete, Construction and Building Materials, 23(2) (2009) 976–980. https://doi.org/10.1016/j.conbuildmat.2008.05.005
22. B. Bhardwaj, P. Kumar, Waste foundry sand in concrete: A review, Construction and Building Materials, 156 (2017) 661–674. https://doi.org/10.1016/j.conbuildmat.2017.09.010
23. Y. Guney, Y.D. Sari, M. Yalcin, A. Tuncan, S. Donmez, Re-usage of waste foundry sand in high-strength concrete, Waste Management, 30(8–9) (2010) 1705–1713. https://doi.org/10.1016/j.wasman.2010.02.018

24. G.G. Prabhu, J.H. Hyun, Y.Y. Kim, Effects of foundry sand as a fine aggregate in concrete production, Construction and Building Materials, 70 (2014) 514–521. https://doi.org/10.1016/j.conbuildmat.2014.07.070
25. N. Gurumoorthy, K. Arunachalam, Micro and mechanical behaviour of treated used foundry sand concrete, Construction and Building Materials, 123 (2016) 184–190. https://doi.org/10.1016/j.conbuildmat.2016.06.143
26. R.K. Sandhu, R. Siddique, Properties of self-compacting concrete incorporating waste foundry sand, Leonardo Journal of Sciences, 12(23) (2013) 105–124.
27. A. Parashar, P. Aggarwal, B. Saini, Y. Aggarwal, S. Bishnoi, Study on performance enhancement of self-compacting concrete incorporating waste foundry sand, Construction and Building Materials, 251 (2020) 118875. https://doi.org/10.1016/j.conbuildmat.2020.118875
28. R.K. Sandhu, R. Siddique, Strength properties and microstructural analysis of self-compacting concrete incorporating waste foundry sand, Construction and Building Materials, 225 (2019) 371–383. https://doi.org/10.1016/j.conbuildmat.2019.07.216
29. D.K. Ashish, S.K. Verma, Robustness of self-compacting concrete containing waste foundry sand and metakaolin: A sustainable approach, Journal of Hazardous Materials, 401 (2021) 123329. https://doi.org/10.1016/j.jhazmat.2020.123329
30. R.K. Sandhu, R. Siddique, Durability performance of self-compacting concrete made with waste foundry sand, Structural Concrete, 23 (2022) 722–738. https://doi.org/10.1002/suco.202100164